

# frontiers in **NEUROENGINEERING**

**This Provisional PDF corresponds to the article as it appeared upon acceptance.**

**Fully formatted PDF and full text (HTML) versions will be made available soon.**

**Visit Frontiers at: [www.frontiersin.org](http://www.frontiersin.org)**

# **Poly(3,4-ethylene dioxythiophene) (PEDOT) as a micro-neural interface material for electrostimulation**

**Seth J. Wilks<sup>1</sup>, Sarah M. Richardson-Burns<sup>2,3</sup>, Jeffery L. Hendricks<sup>3,4</sup>, Dave C. Martin<sup>2,3,4</sup> and Kevin J. Otto<sup>1,5\*</sup>**

1 Weldon School of Biomedical Engineering, Purdue University, USA

2 Department of Materials Science and Engineering, University of Michigan, USA

3 Biotectix, LCC, USA

4 Department of Biomedical Engineering, University of Michigan, USA

5 Department of Biological Sciences, Purdue University, USA

## **Correspondence:**

Dr. Kevin J. Otto

Purdue University

Weldon School of Biomedical Engineering

NeuroProstheses Research Laboratory

206 S. Martin Jischke Dr.

West Lafayette, IN 47907, USA

email: kotto@purdue.edu

## **Running title:**

PEDOT neural interface for electrostimulation

## Abstract

Chronic microstimulation-based devices are being investigated to treat conditions such as blindness, deafness, pain, paralysis and epilepsy. Small area electrodes are desired to achieve high selectivity. However, a major trade-off with electrode miniaturization is an increase in impedance and charge density requirements. Thus, the development of novel materials with lower interfacial impedance and enhanced charge storage capacity is essential for the development of micro-neural interface-based neuroprostheses. In this report, we study the use of conducting polymer poly(3,4-ethylene dioxythiophene) (PEDOT) as a neural interface material for microstimulation of small area iridium electrodes on silicon-substrate arrays. Characterized by electrochemical impedance spectroscopy, electrodeposition of PEDOT results in lower interfacial impedance at physiologically-relevant frequencies, with the 1kHz impedance magnitude being  $23.3 \pm 0.7 \text{ k}\Omega$ , compared to  $113.6 \pm 3.5 \text{ k}\Omega$  for iridium oxide (IrOx) on  $177 \mu\text{m}^2$  sites. Further, PEDOT exhibits enhanced charge storage capacity at  $75.6 \pm 5.4 \text{ mC/cm}^2$  compared to  $28.8 \pm 0.3 \text{ mC/cm}^2$  for IrOx, characterized by cyclic voltammetry (50 mV/s). These improvements at the electrode interface were corroborated by observation of the voltage excursions that result from constant current pulsing. The PEDOT coatings provide both a lower amplitude voltage and a more ohmic representation of the applied current compared to IrOx. During repetitive pulsing, PEDOT-coated electrodes show stable performance and little change in electrical properties, even at relatively high current densities which cause IrOx instability. These findings support the potential of PEDOT coatings as a micro-neural interface material for electrostimulation.

## Keywords

Microelectrode, charge injection, iridium oxide, impedance, cyclic voltammetry

## 1. Introduction

Chronic electrical stimulation of neural tissue has shown considerable promise in treating movement and sensory impairments, especially with deep brain stimulation (DBS) and cochlear implants. While many of these treatments involve low-channel count macrostimulation using large surface area ( $>0.1 \text{ mm}^2$ ) macroelectrodes, the breadth of neural therapies can be increased and improved with more selective microstimulation through small surface area microelectrodes. Chronic microstimulation-based devices have shown potential as auditory (Rousche and Normann, 1999; Rousche *et al.*, 2003; Otto *et al.*, 2005; Lim and Anderson, 2006; McCreery, 2008), visual (Bak *et al.*, 1990; Schmidt *et al.*, 1996; Normann *et al.*, 1999; Bradley *et al.*, 2005; Weiland *et al.*, 2005), somatosensory (Romo and Salinas, 2001; Butovas and Schwarz, 2007), motor control (Mushahwar *et al.*, 2002), and bladder control (Pikov *et al.*, 2007) prostheses. While electrode miniaturization results in high selectivity, a negative side-effect is that the charge density requirements of the electrode material are increased. Consequently, performance of chronic microstimulation-based devices is limited due to both the lack of materials that safely and reliably deliver appropriate charge and the insulating effect of tissue reactions.

Platinum (Pt), iridium (Ir) and alloys of the two (PtIr) rate among the highest in Warburg capacitance (Geddes and Roeder, 2003) and have commonly been used as implantable electrodes for electrostimulation, including deep brain stimulator electrodes and cochlear implants. However, due to low charge injection limits ( $0.05\text{-}0.3 \text{ mC/cm}^2$ ), bare noble metals are often

disregarded as small-area neural stimulation electrode materials (Rose and Robblee, 1990; Cogan *et al.*, 2005). Iridium oxide (IrOx) films display a large electrochemical surface area and the ability to quickly inject reversible charge through electron exchange that occurs during the reversible oxidation and reduction of Ir<sup>3+</sup> and Ir<sup>4+</sup> (Mozota and Conway, 1983). IrOx displays a charge injection limit of 0.9 mC/cm<sup>2</sup> which can be increased to 3.3 mC/cm<sup>2</sup> with the application of voltage-biased asymmetric waveforms (Cogan *et al.*, 2006). However, short-term pulsing results in IrOx instability at charge density levels between 2-3 mC/cm<sup>2</sup>, characterized by damaged IrOx films and Ir fragments in the adjacent tissue (Cogan *et al.*, 2004). Long-term *in vivo* stimulation studies have shown instability in the IrOx electrode-tissue interface, resulting in adverse tissue reactions (Weiland and Anderson, 2000).

Conductive polymers are emerging as neural stimulation materials and exhibit both fast and high charge delivery capacities due to high ionic conductivity and a large electroactive surface area (Ghosh and Inanas, 2000). These properties lead to very low impedance and highly effective charge transfer (Abidian and Martin, 2008). Poly(3,4-ethylene dioxythiophene) (PEDOT) coatings on neural electrodes have been reported to display charge injection limits similar to IrOx at 2.3-3.6 mC/cm<sup>2</sup> (Cui and Zhou, 2007; Nyberg *et al.*, 2007) and much higher than IrOx at approximately 15 mC/cm<sup>2</sup> (Cogan, 2008). Thin PEDOT coatings have demonstrated electrochemical stability during long-term stimulation at charge densities of 0.35 mC/cm<sup>2</sup> in PBS (Cui and Zhou, 2007). Further, bioactive molecules can be incorporated into PEDOT films (Cui and Martin, 2003; Abidian *et al.*, 2006; Kim *et al.*, 2007) and PEDOT can be polymerized in and around living neural tissue, signifying the possibility of a hybrid polymer-live cell electrode (Richardson-Burns *et al.*, 2007b; Richardson-Burns *et al.*, 2007a). This report examines PEDOT as a micro-neural interface material for electrical stimulation. Electrochemically deposited PEDOT and activated IrOx coatings on small-area Ir electrode arrays were used. The coatings were characterized by scanning electron microscopy (SEM), electrochemical impedance spectroscopy (EIS), cyclic voltammetry (CV), and voltage excursion measurements. The effects of short-term application of relevant charge densities on coating stability were also characterized.

## 2. Materials and methods

### 2.1. Microelectrode arrays

Microfabricated silicon-substrate electrode arrays used in this study were provided by the University of Michigan Center for Neural Communication Technology (CNCT). The arrays consisted of four 15  $\mu\text{m}$  thick silicon shanks spaced 125  $\mu\text{m}$  apart with four thin-film Ir sites on each shank. Sites diameters were either 15  $\mu\text{m}$  or 23  $\mu\text{m}$ , resulting in a site area of 177  $\mu\text{m}^2$  or 413  $\mu\text{m}^2$ . The electrodes were activated to form IrOx or electrochemically deposited with PEDOT as described below. An FEI Quanta 3D FEG field emission SEM (FEI Company Inc, Hillsboro, OR) was used to study the surface morphology of IrOx and PEDOT coated sites. SEM images were taken using a LVED detector in low vacuum mode (0.9 T) with a voltage of 15kV and spot size of 6.

### 2.2. Electrochemical measurements

Electrochemical measurements were made using an Autolab Potentiostat/Galvonostat PG-STAT12 (Eco Chemie, Utrecht, Netherlands) with a built-in frequency response analyzer (Brinkmann, Westbury, NY). A three-electrode cell configuration in 1X phosphate buffered

saline (PBS) having a concentration of 154 mM NaCl, 5.8 mM NaH<sub>2</sub>PO<sub>4</sub> and 1.1 mM KH<sub>2</sub>PO<sub>4</sub> was used. The microelectrode site functioned as the working electrode (WE), a large-area Pt wire functioned as the counter electrode (CE), and an Accumet, gel-filled, KCl saturated calomel electrode (SCE) (Thermo Fischer Scientific, Fair Lawn, NJ) functioned as the reference electrode (RE).

EIS measurements were collected by configuring the Autolab to sequentially inject overpotentials of 5 mV<sub>RMS</sub> sine waves at 36 frequencies logarithmically spaced from 1 Hz to 1 MHz. CV measurements were collected by configuring the Autolab to sweep the voltage of the WE at a constant rate within the potential limits of hydrolysis and monitor the resulting current flow between the WE and CE. The potential limits used for Ir and IrO<sub>x</sub> was +0.8 V to -0.6 V while that for PEDOT was +0.6 V to -0.8 V. Both slow (50 mV/s) and fast (1 V/s) sweep rates were used to assess the static equilibrium at each voltage point and the charge available at the exposed area of the microelectrode site. The CV measurements were used to evaluate electrochemical reactions at the interface, double layer charging, and the cathodal charge storage capacity ( $Q_{cap}$ ). The location of peaks in the CV indicate potentials where oxidation and reduction reactions are occurring, peak amplitudes indicate the amount of charge carriers at the interface and the  $Q_{cap}$  is a measure of the charge available at the electrode interface.  $Q_{cap}$  was calculated by integrating the cathodal current density enclosed by the CV and dividing by the sweep rate.

### 2.3. IrO<sub>x</sub> and PEDOT coatings

IrO<sub>x</sub> was activated on bare Ir sites using the Autolab Potentiostat/Galvonostat and three-electrode setup described previously. The activation performed in this report is a well established technique that has been described in detail elsewhere (Robblee *et al.*, 1983). In brief, activation involved applying 1-Hz voltage pulses with an anodic potential of +0.8 V followed by a cathodic potential of -0.9 V. This was done for 1600 s in 1X PBS to result in a  $Q_{cap}$  of approximately 30 mC/cm<sup>2</sup>.

PEDOT coatings used in this study were provided by Biotectix, LCC. PEDOT was deposited on the microelectrode sites by electrochemical polymerization. The electrode was placed in an electrically-connected reservoir containing the aqueous monomer solution comprised of 0.01 M EDOT (Bayer/HC Starck) in deionized water with 2.5 mg/ml polyanionic poly(sodium styrene sulfonate) (PSS; Sigma-Aldrich). A platinum foil served as the CE and an electrode site of the neural probe was the WE. Galvanostatic electrodeposition was used to form the polymer on electrode sites using 2-10 mA/cm<sup>2</sup>. Current was passed between the WE and the CE in the monomer solution using an Autolab Potentiostat/Galvonostat PGSTAT12 for 300-900 sec (exact duration was determined empirically according to desired film thickness).

### 2.4. Electrical stimulation

Electrical stimulation was delivered via a programmable multichannel microstimulator system (Tucker-Davis Technologies, Alachua, FL) in 1X PBS. Cathodal-first, charge-balanced, biphasic current pulses were applied between the microelectrode site and a large-area Pt wire. The current amplitude was chosen as the maximum current that could be safely applied without inducing neural damage, determined by the following equation

$$Q = \sqrt{A * 10^k}$$

where  $Q$  is charge per phase in  $\mu\text{C}$ ,  $A$  is the electrode surface area in  $\text{cm}^2$ , and  $k$  is a constant of 1.7 (Shannon, 1992). Using 200  $\mu\text{s}$  phase durations, the maximum amplitude is approximately 45  $\mu\text{A}$  for 177  $\mu\text{m}^2$  surface area electrodes (charge density of 5  $\text{mC}/\text{cm}^2$ ) and 70  $\mu\text{A}$  for 413  $\mu\text{m}^2$  surface area electrodes (charge density of 3.4  $\text{mC}/\text{cm}^2$ ). In this study, pulses were delivered at these maximum amplitudes continuously at 100 Hz for 2 hours (720,000 pulses). The resulting voltage excursions were measured with respect to the Pt counter electrode during current pulsing in order to assess the safety and efficacy of the interface during charge transfer.

## 2.5. Statistics

Student's t-tests were used to evaluate the statistical significance in all datasets,  $P < 0.05$ . All error-bar regions represent standard error mean from  $n = 9$  sites (177  $\mu\text{m}^2$ ) from three different arrays for IrOx and  $n = 4$  sites (177  $\mu\text{m}^2$ ) from one array for PEDOT.

## 3. Results

### 3.1. Electrode surface morphology

Figures 1A and C show SEM images of IrOx and PEDOT coatings on the Ir electrode sites (413  $\mu\text{m}^2$ ). The IrOx coatings display a slightly rough surface (figure 1B) with noticeable cracks along the edge of the electrode site. The PEDOT coatings are much thicker and a dense arrangement of submicron sized clumps appear to uniformly cover the entire electrode site (figure 1D).

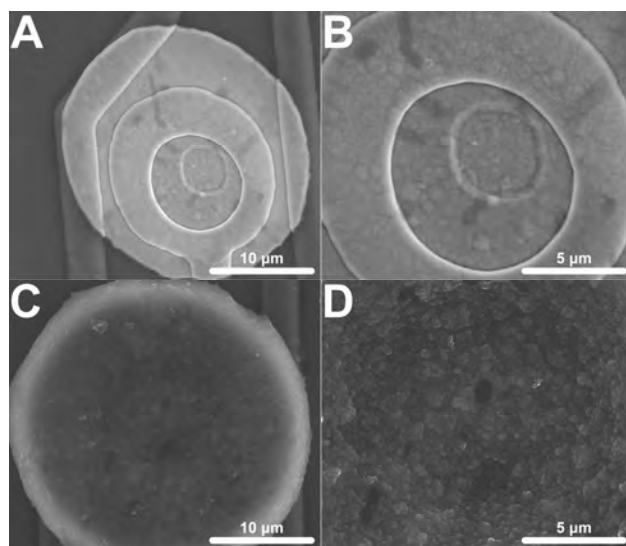


Figure 1. Scanning electron microscopy (SEM) images of electrode surfaces (413  $\mu\text{m}^2$ ). (A) An overall coating and (B) microscale surface morphology of IrOx which was activated by biasing bare Ir between +0.8 V and -0.9 V at 1 Hz for 1600 s is shown. (C) An overall coating and (D) microscale surface morphology of PEDOT which was galvanostatically deposited at 2 nA for 1200 s is shown.

### 3.2. Electrochemical measurements

The complex impedance magnitude for the Ir microelectrodes greatly decreased after IrOx and PEDOT deposition. Mean impedance magnitude for IrOx was significantly less than Ir for all frequencies below 10 kHz and PEDOT displayed a lower impedance magnitude than both Ir and IrOx for all frequencies (figure 2A). Low phase values near zero indicate highly resistive impedance and high phase values near -90 indicate highly capacitive impedance. Phase values for IrOx were significantly lower than Ir at all frequencies below 100 kHz and PEDOT displayed a lower phase value than both Ir and IrOx for all frequencies above 10 Hz, representing a more resistive interface (figure 2B). 1 kHz impedance magnitudes are particularly important due to the biological relevance of action potentials having a fundamental frequency of 1 kHz. Bare Ir, IrOx and PEDOT surfaces displayed 1 kHz impedance values of  $404.5 \pm 15.2 \text{ k}\Omega$ ,  $113.6 \pm 3.5 \text{ k}\Omega$  and  $23.3 \pm 0.7 \text{ k}\Omega$  (figure 2C).

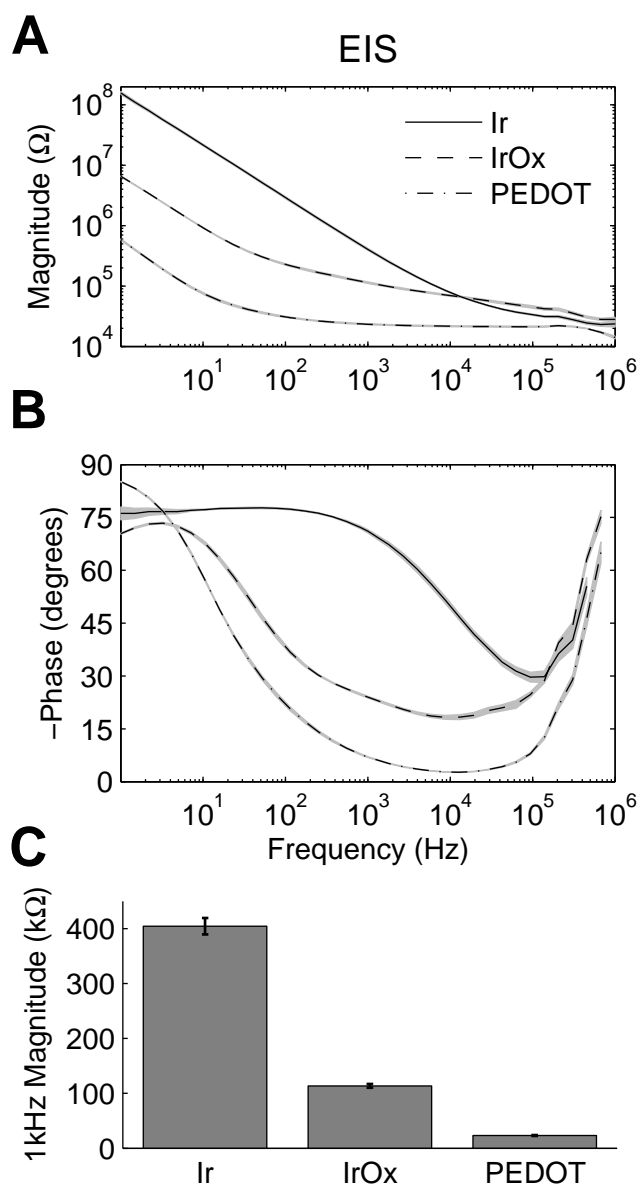


Figure 2. Electrochemical impedance spectroscopy (EIS) measurements. (A) Mean impedance magnitude and (B) phase measurements for 36 frequencies logarithmically spaced between 1Hz and 1 MHz are shown. (C) Mean 1kHz impedance magnitudes were significantly less for IrOx and PEDOT coated sites.

The CV data provide information on the charge transfer properties of the electrode interface. IrOx charge transfer is highly faradaic in behavior corresponding to the distinct peaks associated with the reversible oxidation and reduction of Ir (figure 3A,C). PEDOT charge transfer is also faradaic and additionally displays a large rectangular shape for the fast sweep rate (1 V/s) CV, indicating high capacitive charge transfer. Mean  $Q_{cap}$  values were calculated from these CV data to quantify the charge available at each material interface and resulted in the following fashion: Ir < IrOx < PEDOT (figure 3B,D). The  $Q_{cap}$  for IrOx was  $28.8 \pm 0.3$  mC/cm<sup>2</sup> for the slow sweep rate CV and  $17.6 \pm 0.2$  mC/cm<sup>2</sup> for the fast sweep rate CV while that for PEDOT was  $75.6 \pm 5.4$  mC/cm<sup>2</sup> and  $178.5 \pm 5.3$  mC/cm<sup>2</sup>. Interestingly, the  $Q_{cap}$  for PEDOT measured from the fast sweep rate CV was much higher than that calculated from the slow sweep rate CV, which could be beneficial for charge transfer during physiologically relevant electrical stimulation.

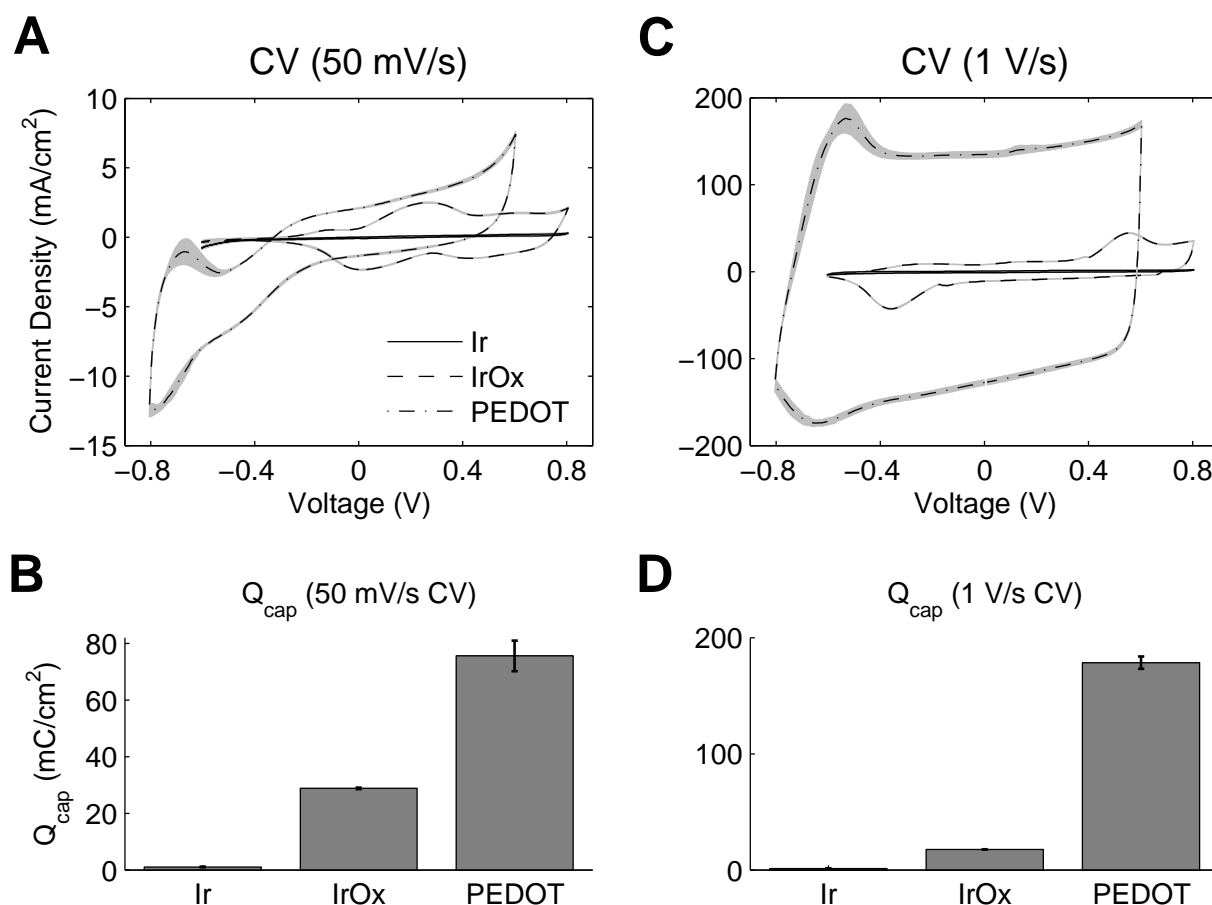


Figure 3. Cyclic voltammetry (CV) measurements. Both (A) slow (50 mV/s) and (B) fast (1 V/s) sweep rates show PEDOT coated electrodes with much larger CV areas than IrOx and bare Ir. (C,D) Mean charge storage capacities ( $Q_{cap}$ ) calculated by integrating the cathodal current area



enclosed by the CV divided by the sweep rate show that PEDOT has more charge available at the interface.

### 3.3. Electrical stimulation

Cathodal-first, charge-balanced, biphasic current pulses are frequently used for effective and safe stimulation of neural tissue (Lilly *et al.*, 1955; Brummer and Turner, 1975; Merrill *et al.*, 2005). Measuring the corresponding voltage excursion is commonly employed to calculate the safe charge injection limits of the interface. Ir and IrOx voltage excursions display an initial ohmic voltage drop followed by a more gradual polarization of the interface (figure 4). Due to increased charge carriers at the interface, less polarization is seen at the IrOx interface compared to Ir. PEDOT displayed a much lower initial ohmic voltage drop which was not followed by additional polarization. The PEDOT voltage excursion displayed a very ohmic representation of the current delivered which corresponded closely to its 1 kHz impedance value. By employing Ohm's law, a current of 45  $\mu\text{A}$  delivered across a 23.3 k $\Omega$  resistor results in a voltage of 1.05 V and the mean cathodal voltage drop for PEDOT with respect to its zero current potential was 1.14 V. The relatively low voltage amplitude and ohmic representation of the PEDOT voltage excursion is indicative of improved charge injection limits compared to IrOx.

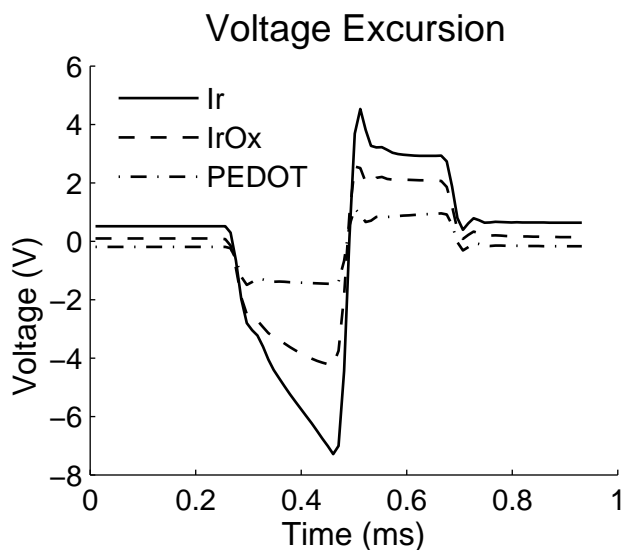


Figure 4. Voltage excursion data taken from biphasic current pulses with 200  $\mu\text{s}$  phase durations, and 45  $\mu\text{A}$  amplitudes resulting in a charge density of 5  $\text{mC}/\text{cm}^2$ . These data are taken from 177  $\mu\text{m}^2$  surface area electrodes.

IrOx and PEDOT coated electrodes were pulsed at charge densities of approximately 5  $\text{mC}/\text{cm}^2$  (177  $\mu\text{m}^2$ ) and 3.4  $\text{mC}/\text{cm}^2$  (413  $\mu\text{m}^2$ ) which has been previously reported to cause IrOx delamination (Cogan *et al.*, 2004). Pulsing IrOx resulted in a significant increase in the impedance magnitude at all frequencies below 200 kHz (figure 5A) and a significant increase in phase at all frequencies above 30 Hz (figure 5B). The 1 kHz impedance magnitude increased from  $113.6 \pm 3.5$  k $\Omega$  to  $183.9 \pm 12.5$  k $\Omega$  (figure 5C). Slow sweep rate CVs displayed large anodic peaks around 0.6-0.7 V after pulsing demonstrating pulse-induced activation (figure 5D). The oxidation-reduction peaks seen in the fast sweep rate CVs were greatly reduced after pulsing indicating that a lower amount of charge carriers were available at the interface (figure 5E).

Mean  $Q_{\text{cap}}$  values calculated from the slow sweep rate CVs showed a significant increase from  $28.8 \pm 0.3 \text{ mC/cm}^2$  to  $35.1 \pm 1.1 \text{ mC/cm}^2$  while values calculated from the fast sweep rate CVs show a significant decrease from  $17.6 \pm 0.2 \text{ mC/cm}^2$  to  $14.1 \pm 0.3 \text{ mC/cm}^2$  (figure 5F).

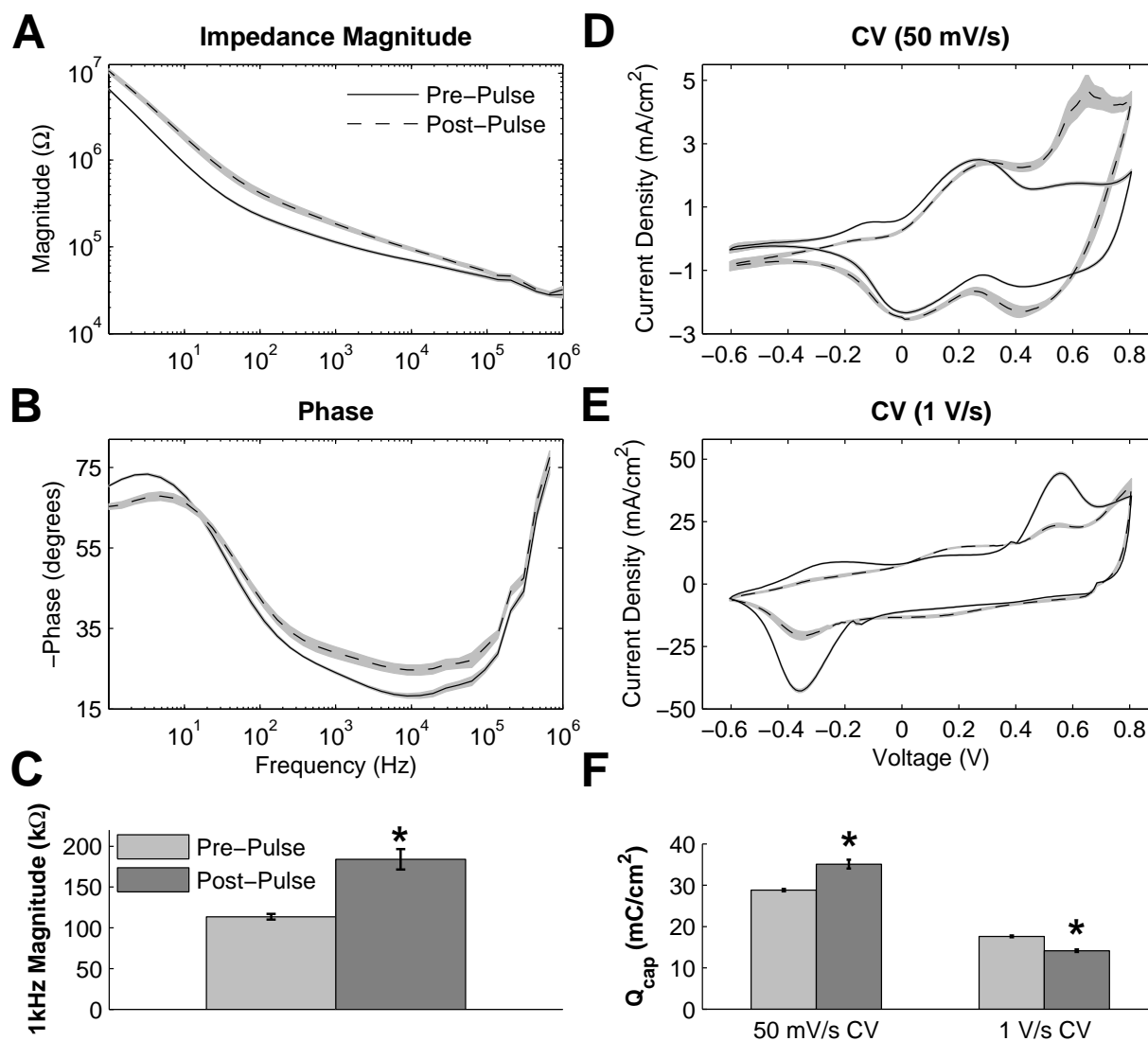


Figure 5. Effects of continuously pulsing (200  $\mu\text{s}$  phase duration, 45  $\mu\text{A}$  amplitude, 100 Hz) IrOx coated electrodes ( $177 \mu\text{m}^2$ ) for 2 hours. (A) Mean impedance and (B) phase changed significantly for nearly all frequencies after pulsing. (C) The 1kHz impedance magnitude increased significantly indicating IrOx delamination. (D) Slow CV measurements show pulse induced IrOx activation while (E) fast CV measurements show IrOx degradation. (F) These changes in the CV correspond to an increase in  $Q_{\text{cap}}$  for the slow CV measurements and a decrease in  $Q_{\text{cap}}$  for fast CV measurements.

The PEDOT coatings were examined during the same pulsing protocol used to assess the IrOx coatings. Almost identical pre- and post-pulsing impedance magnitude and phase plots were seen at all frequencies below 100 kHz (figure 6A,B). Pulsing PEDOT resulted in no significant difference in the 1 kHz impedance magnitude (figure 6C). The pre- and post-pulsing CVs

displayed slight changes with decreases in the mean  $Q_{\text{cap}}$  from  $75.6 \pm 5.4 \text{ mC/cm}^2$  to  $71.6 \pm 5.3 \text{ mC/cm}^2$  for the slow sweep rate CV and from  $178.5 \pm 5.4 \text{ mC/cm}^2$  to  $166.5 \pm 5.6 \text{ mC/cm}^2$  for the fast sweep rate CV (figure 6D-F). However, no statistical difference was observed for the  $Q_{\text{cap}}$  values before and after pulsing. The PEDOT coatings remained electrochemically stable during short-term pulsing. The pre- and post-pulsing values for IrOx and PEDOT coated sites are summarized in table 1.

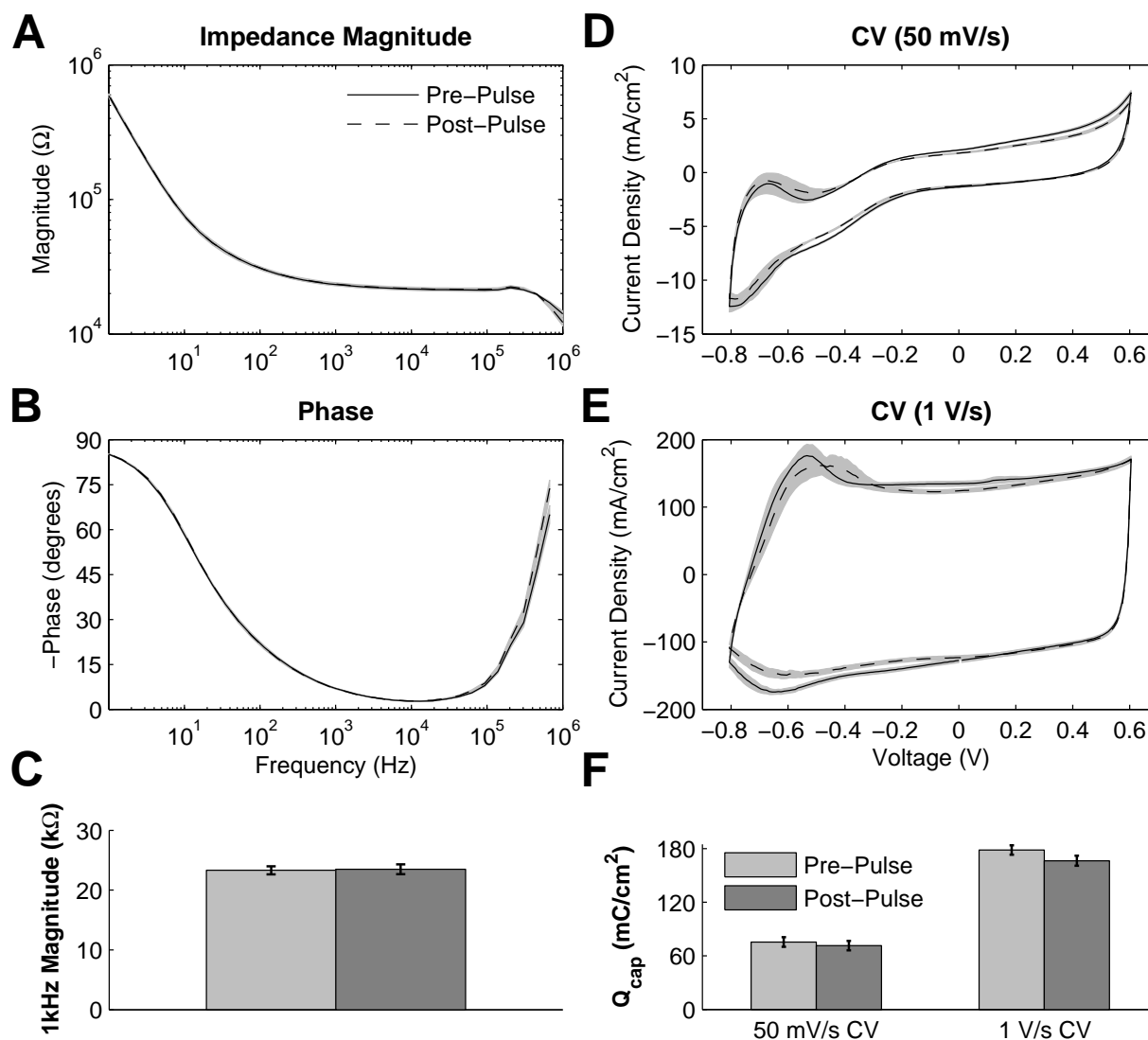


Figure 6. Effects of continuously pulsing ( $200 \mu\text{s}$  phase duration,  $45 \mu\text{A}$  amplitude,  $100 \text{ Hz}$ ) PEDOT coated electrodes ( $177 \mu\text{m}^2$ ) for 2 hours. (A) Mean impedance magnitude and (B) phase showed no significant change between pre-stimulation and post-stimulation values at all frequencies. (C) This is seen by comparing the 1kHz impedance magnitudes. Both (D) slow and (E) fast CV measurements show little change after pulsing and (F) there is no significant change in the  $Q_{\text{cap}}$ .

**Table 1: Pre- and post pulsing properties**

Interface Material	1 kHz impedance (k $\Omega$ )		$Q_{cap}$ (mC/cm $^2$ )*	
	pre-pulsing	post-pulsing	pre-pulsing	post-pulsing
Ir	404.5 $\pm$ 15.2	—	1.1 $\pm$ 0.1	—
IrOx	113.6 $\pm$ 3.5	183.9 $\pm$ 12.5	28.8 $\pm$ 0.3	35.1 $\pm$ 1.1
PEDOT	23.3 $\pm$ 0.7	23.5 $\pm$ 0.8	75.6 $\pm$ 5.4	71.6 $\pm$ 5.3

\*Values calculated from 50 mV/s sweep rate CV

Similar increases in impedance and  $Q_{cap}$  were seen for the larger surface area (413  $\mu\text{m}^2$ ) IrOx coated sites pulsed at 3.4 mC/cm $^2$  which caused extensive damage to the IrOx coating (figure 7). Almost no change was observed with the PEDOT coated sites pulsed at the same levels. These data confirm that the threshold for IrOx delamination is below 3.4 mC/cm $^2$ , which occurs within only two hours of current pulsing. Alternatively, PEDOT coatings remain stable at electrostimulation levels which cause IrOx damage.

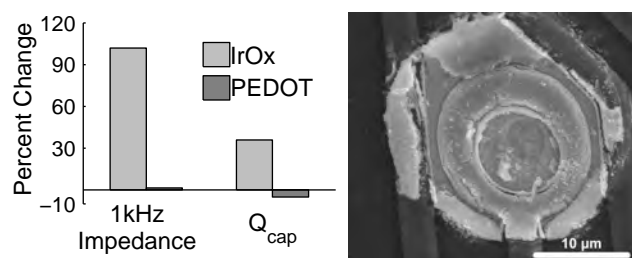


Figure 7. Effects of continuously pulsing (200  $\mu\text{s}$  phase duration, 70  $\mu\text{A}$  amplitude, 100 Hz) IrOx and PEDOT coated electrodes (413  $\mu\text{m}^2$ ) for 2 hours characterized by the change in 1kHz impedance and  $Q_{cap}$ . The SEM image of a pulsed IrOx site shows an extensively damaged coating.

#### 4. Discussion

IrOx has been compared with metal-based materials such as PtIr (Cogan *et al.*, 2005) and TiN (Weiland *et al.*, 2002), and currently is considered the best interface material for neural stimulation. Many studies have suggested the conductive polymer PEDOT as a microelectrode coating for neural stimulation due to its desirable electrical properties (Cui and Martin, 2003; Guimard *et al.*, 2007; Abidian and Martin, 2008), electrochemical stability (Kros *et al.*, 2005) and ability for biomolecule immobilization (Cui and Martin, 2003; Abidian *et al.*, 2006; Kim *et al.*, 2007; Abidian and Martin, 2008), but direct comparisons with IrOx coatings have yet to be reported. The results presented in this report suggest PEDOT is a superior micro-neural interface material for electrostimulation compared to IrOx. PEDOT exhibits much lower interfacial impedance across the entire spectrum which has many implications for both recording and stimulating applications. Lower impedance results in higher signal-to-noise ratios (SNR) for improved electrophysiological recordings and a more effective interface for constant-current stimulation.

The large rectangular CV curve for PEDOT coated electrodes is representative of more charge available for electrical stimulation corresponding with the increased surface area seen in SEM images and indicative of fast ion transport across the PEDOT coating. PEDOT  $Q_{cap}$  values are

more than double that of IrOx, analogous to more charge available at the interface. Only a small portion of the  $Q_{\text{cap}}$  is accessible for charge injection during fast current pulsing, but higher  $Q_{\text{cap}}$  results in higher charge injection capacities corresponding to lower voltage excursions during constant current pulsing. PEDOT voltage excursions are much smaller in amplitude than IrOx and are very ohmic in their shape. The ability to push current at lower voltage amplitudes reduces the formation of toxic species and lowers power consumption of the microstimulator device.

The chronic functionality of neural prostheses is dependent on maintaining a stable electrode-tissue interface. During electrical stimulation, properties of the neural interface material must not degrade or create foreign species. Consistent with previous reports, repetitive pulsing that results in large voltage excursions causes unstable IrOx activation and delamination. This damages the electrode material and will most likely cause tissue damage, greatly compromising the quality of the neural interface. As a result of pulsing, the interfacial impedance is significantly increased after only two hours. PEDOT displayed a much more stable interface for repetitive pulsing and no changes were observed in the complex impedance spectra. A slight loss in  $Q_{\text{cap}}$  occurred, but since there was no change in impedance, this is most likely due to rearrangement of the PEDOT and PSS structure after sweeping the voltage during the CV measurement (Cui and Martin, 2003).

The data presented in this report suggests that PEDOT is better suited than IrOx as a micro-neural interface material for delivering physiologically relevant stimulation. PEDOT exhibits lower interfacial impedance, higher  $Q_{\text{cap}}$  and lower amplitude voltage excursions which are more ohmic in shape than that exhibited by IrOx. Further, the electrochemical properties of PEDOT coatings remain stable and reliable after short-term repetitive pulsing at current densities IrOx is unable to handle. While these results are promising, long-term stability and *in vivo* evaluation is still necessary to further suggest PEDOT for chronically implantable and functional coatings.

### **Conflict-of-interest statement**

Sarah M. Richardson-Burns, Jeffrey L. Hendricks and David C. Martin have financial interest in Biotectix, LCC, an innovator in the development and use of conductive polymer materials and coatings. This conflict of interest is managed by the University of Michigan.

### **Acknowledgements**

This work was supported by the Purdue Research Foundation. The authors would like to thank the Purdue NeuroProstheses Research lab for helping in the preparation of this manuscript, the Center for Neural Communication Technology for providing microelectrode arrays (NIH/NIBIB P41-EB002030), Biotectix, LCC for providing the PEDOT coatings and the Purdue Life Science Microscopy Facility for assisting in acquiring SEM images.

### **References**

Abidian, M. R., Martin, D. C. (2008). Experimental and theoretical characterization of implantable neural microelectrodes modified with conducting polymer nanotubes. *Biomaterials* 29, 1273-1283.

- Abidian, M. R., Kim, D. H., Martin, D. C. (2006). Conding-polymer nanotubes for controlled drug release. *Adv. Mater.* 18, 405-409.
- Bak, M., Girvin, J. P., Hambrecht, F. T., Kufta, C. V., Loeb, G. E., Schmidt, E. M. (1990). Visual sensations produced by intracortical microstimulation of the human occipital cortex. *Med. Biol. Eng. Comput.* 28, 257-259.
- Bradley, D. C., Troyk, P. R., Berg, J. A., Bak, M., Cogan, S., Erickson, R., Kufta, C., Mascaro, M., McCreery, D., Schmidt, E. M., Towle, V. L., Xu, H. (2005). Visuotopic mapping through a multichannel stimulating implant in primate V1. *J. Neurophysiol.* 93, 1659-1670.
- Brummer, S. B., Turner, M. J. (1975). Electrical stimulation of the nervous system: The principle of safe charge injection with noble metal electrodes. *Bioelectrochem. Bioenerg.* 2, 13-25.
- Butovas, S., Schwarz, C. (2007). Detection psychophysics of intracortical microstimulation in rat primary somatosensory cortex. *Eur. J. Neurosci.* 25, 2161-2169.
- Cogan, S. F. (2008). Neural stimulation and recording electrodes. *Annu. Rev. Biomed. Eng.* 10, 275-309.
- Cogan, S. F., Troyk, P. R., Ehrlich, J., Plante, T. D. (2005). In vitro comparison of the charge-injection limits of activated iridium oxide (AIROF) and platinum-iridium microelectrodes. *IEEE Trans. Biomed. Eng.* 52, 1612-1614.
- Cogan, S. F., Guzelian, A. A., Agnew, W. F., Yuen, T. G., McCreery, D. B. (2004). Over-pulsing degrades activated iridium oxide films used for intracortical neural stimulation. *J. Neurosci. Methods* 137, 141-150.
- Cogan, S. F., Troyk, P. R., Ehrlich, J., Plante, T. D., Detlefsen, D. E. (2006). Potential-biased, asymmetric waveforms for charge-injection with activated iridium oxide (AIROF) neural stimulation electrodes. *IEEE Trans. Biomed. Eng.* 53, 327-332.
- Cui, X. T., Zhou, D. D. (2007). Poly (3,4-ethylenedioxythiophene) for chronic neural stimulation. *IEEE Trans. Neural Syst. Rehabil. Eng.* 15, 502-508.
- Cui, X. Y., Martin, D. C. (2003). Electrochemical deposition and characterization of poly (3,4-ethylenedioxythiophene) on neural microelectrode arrays. *Sensors Actuators B-Chemical* 89, 92-102.
- Geddes, L. A., Roeder, R. (2003). Criteria for the selection of materials for implanted electrodes. *Ann. Biomed. Eng.* 31, 879-890.
- Ghosh, S., Inngan, O. (2000). Electrochemical characterization of poly(3,4-ethylene dioxythiophene) based conducting hydrogel networks. *J. Electrochem. Soc.* 147, 1872-1877.
- Guimard, N. K., Gomez, N., Schmidt, C. E. (2007). Conducting polymers in biomedical engineering. *Prog. Polym. Sci.* 32, 876-921.
- Kim, D. H., Richardson-Burns, S. M., Hendricks, J. L., Sequera, C., Martin, D. C. (2007). Effect of immobilized nerve growth factor on conductive polymers: electrical properties and cellular response. *Adv. Func. Mater.* 17, 79-86.
- Kros, A., Sommerdijk, N. A. J. M., Nolte, R. J. M. (2005). Poly(pyrrole) versus poly(3,4-ethylenedioxythiophene): implications for biosensor applications. *Sensors Actuators B-Chemical* 106, 289-295.
- Lilly, J. C., Hughes, J. R., Alvord, E. C., Jr., Galkin, T. W. (1955). Brief, noninjurious electric waveform for stimulation of the brain. *Science* 121, 468-469.

- Lim, H. H., Anderson, D. J. (2006). Auditory cortical responses to electrical stimulation of the inferior colliculus: implications for an auditory midbrain implant. *J. Neurophysiol.* 96, 975-988.
- McCreery, D. B. (2008). Cochlear nucleus auditory prostheses. *Hear. Res.* 242, 64-73.
- Merrill, D. R., Bikson, M., Jefferys, J. G. (2005). Electrical stimulation of excitable tissue: design of efficacious and safe protocols. *J. Neurosci. Methods* 141, 171-198.
- Mozota, J., Conway, B. E. (1983). Surface and bulk processes at oxidized iridium electrodes - I. Monolayer stage and transition to reversible multilayer oxide film behaviour. *Electrochimica Acta* 28, 1-8.
- Mushahwar, V. K., Gillard, D. M., Gauthier, M. J., Prochazka, A. (2002). Intraspinal micro stimulation generates locomotor-like and feedback-controlled movements. *IEEE Trans. Neural Syst. Rehabil. Eng.* 10, 68-81.
- Normann, R. A., Maynard, E. M., Rousche, P. J., Warren, D. J. (1999). A neural interface for a cortical vision prosthesis. *Vision Res.* 39, 2577-2587.
- Nyberg, T., Shimada, A., Torimitsu, K. (2007). Ion conducting polymer microelectrodes for interfacing with neural networks. *J. Neurosci. Methods* 160, 16-25.
- Otto, K. J., Rousche, P. J., Kipke, D. R. (2005). Microstimulation in auditory cortex provides a substrate for detailed behaviors. *Hear. Res.* 210, 112-117.
- Pikov, V., Bullara, L., McCreery, D. B. (2007). Intraspinal stimulation for bladder voiding in cats before and after chronic spinal cord injury. *J. Neural Eng.* 4, 356-368.
- Richardson-Burns, S. M., Hendricks, J. L., Martin, D. C. (2007a). Electrochemical polymerization of conducting polymers in living neural tissue. *J. Neural Eng.* 4, L6-L13.
- Richardson-Burns, S. M., Hendricks, J. L., Foster, B., Povlich, L. K., Kim, D. H., Martin, D. C. (2007b). Polymerization of the conducting polymer poly(3,4-ethylenedioxythiophene) (PEDOT) around living neural cells. *Biomaterials* 28, 1539-1552.
- Robblee, L. S., Lefko, J. L., Brummer, S. B. (1983). Activated Ir: An electrode suitable for reversible charge injection in saline solution. *J. Electrochem. Soc.* 130, 731-733.
- Romo, R., Salinas, E. (2001). Touch and go: decision-making mechanisms in somatosensation. *Annu. Rev. Neurosci.* 24, 107-137.
- Rose, T. L., Robblee, L. S. (1990). Electrical stimulation with Pt electrodes. VIII. Electrochemically safe charge injection limits with 0.2 ms pulses. *IEEE Trans. Biomed. Eng.* 37, 1118-1120.
- Rousche, P. J., Normann, R. A. (1999). Chronic intracortical microstimulation (ICMS) of cat sensory cortex using the Utah Intracortical Electrode Array. *IEEE Trans. Rehabil. Eng.* 7, 56-68.
- Rousche, P. J., Otto, K. J., Reilly, M. P., Kipke, D. R. (2003). Single electrode micro-stimulation of rat auditory cortex: an evaluation of behavioral performance. *Hear. Res.* 179, 62-71.
- Schmidt, E. M., Bak, M. J., Hambrecht, F. T., Kufta, C. V., O'Rourke, D. K., Vallabhanath, P. (1996). Feasibility of a visual prosthesis for the blind based on intracortical microstimulation of the visual cortex. *Brain* 119 (Pt 2), 507-522.
- Shannon, R. V. (1992). A model of safe levels for electrical stimulation. *IEEE Trans. Biomed. Eng.* 39, 424-426.

- Weiland, J. D., Anderson, D. J. (2000). Chronic neural stimulation with thin-film, iridium oxide electrodes. *IEEE Trans. Biomed. Eng.* 47, 911-918.
- Weiland, J. D., Anderson, D. J., Humayun, M. S. (2002). In vitro electrical properties for iridium oxide versus titanium nitride stimulating electrodes. *IEEE Trans. Biomed. Eng.* 49, 1574-1579.
- Weiland, J. D., Liu, W., Humayun, M. S. (2005). Retinal prosthesis. *Annu. Rev. Biomed. Eng.* 7, 361-401.